

Rescue of K12G Triosephosphate Isomerase by Ammonium Cations: The Reaction of an Enzyme in Pieces

Maybelle K. Go, Tina L. Amyes, and John P. Richard*

Department of Chemistry, University at Buffalo, SUNY, Buffalo, New York 14260-3000

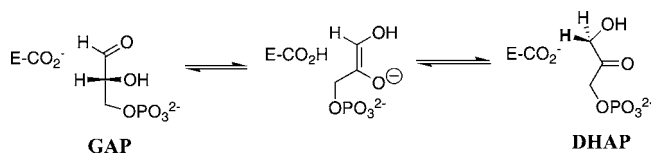
Received July 9, 2010; E-mail: jrichard@buffalo.edu

Abstract: The K12G mutation at yeast triosephosphate isomerase (TIM) results in a 5.5×10^5 -fold decrease in $k_{\text{cat}}/K_{\text{m}}$ for isomerization of glyceraldehyde 3-phosphate, and the activity of this mutant can be successfully “rescued” by NH_4^+ and primary alkylammonium cations. The transition state for the K12G mutant TIM-catalyzed reaction is stabilized by 1.5 kcal/mol by interaction with NH_4^+ . The larger 3.9 kcal/mol stabilization by $\text{CH}_3\text{CH}_2\text{CH}_2\text{CH}_2\text{NH}_3^+$ is due to hydrophobic interactions between the mutant enzyme and the butyl side chain of the cation activator. There is no significant transfer of a proton from alkylammonium cations to GAP at the transition state for the K12G mutant TIM-catalyzed reaction, because activation by a series of RNH_3^+ shows little or no dependence on the $\text{p}K_{\text{a}}$ of RNH_3^+ . A comparison of $k_{\text{cat}}/K_{\text{m}} = 6.6 \times 10^6 \text{ M}^{-1} \text{ s}^{-1}$ for the wildtype TIM-catalyzed isomerization of GAP and the third-order rate constant of $150 \text{ M}^{-2} \text{ s}^{-1}$ for activation by NH_4^+ of the K12G mutant TIM-catalyzed isomerization shows that stabilization of the bound transition state by the effectively intramolecular interaction of the cationic side chain of Lys-12 at wildtype TIM is 6.3 kcal/mol greater than that for the corresponding intermolecular interaction of NH_4^+ at K12G mutant TIM.

Introduction

Triosephosphate isomerase (TIM) catalyzes the stereospecific, reversible 1,2-hydrogen shift at dihydroxyacetone phosphate (DHAP) to give (*R*)-glyceraldehyde 3-phosphate (GAP) by a single-base (carboxylate side chain of Glu-165) proton transfer mechanism through an enzyme-bound *cis*-enediolate intermediate (Scheme 1),^{1,2} which is stabilized by a hydrogen bond between the enediolate oxyanion and the neutral imidazole side chain of His-95.³ Although the *chemical* mechanism for catalysis of deprotonation of α -carbonyl carbon by TIM is similar to that observed for catalysis of this reaction by small Brønsted bases in solution,^{4,5} the basicity of the Glu-165 carboxylate side chain may be greatly enhanced by the protein catalyst.^{3,6} The second-order rate constant $k_{\text{cat}}/K_{\text{m}} = 2.4 \times 10^8 \text{ M}^{-1} \text{ s}^{-1}$ for TIM-catalyzed isomerization of the free carbonyl form of GAP is 4×10^{10} -fold larger than $k_{\text{B}} = 6.5 \times 10^{-3} \text{ M}^{-1} \text{ s}^{-1}$ for deprotonation of GAP by the small tertiary amine quinuclidinone.^{7,8} This shows that interactions with the protein catalyst stabilize the transition state for general-base-catalyzed deprotonation of GAP by ca. 14 kcal/mol.⁸

Scheme 1



Two charged groups, one derived from substrate and the second from the enzyme, are utilized in stabilization of the transition state for TIM-catalyzed proton transfer. First, a comparison of $k_{\text{cat}}/K_{\text{m}}$ for isomerization of GAP with that for enzyme-catalyzed deprotonation of glyceraldehyde shows that interactions between TIM and the substrate phosphodianion group stabilize the transition state by 12 kcal/mol.^{8,9} Second, a comparison of $k_{\text{cat}}/K_{\text{m}}$ for isomerization of GAP by wildtype and K12G mutant TIM shows that interactions with the side chain of Lys-12 stabilize the transition state by 7.8 kcal/mol.³ There is good evidence that this stabilization is due to *electrostatic* interactions between the tethered cationic side chain of Lys-12 and the enediolate-like transition state for the isomerization reaction and that this includes interactions with both the phosphodianion group and the developing negative charge at the enolate oxyanion (Figure 1).^{3,10–12}

Solvent water strongly attenuates electrostatic interactions between dissolved ions. For example, Gibbs free energies of

- (1) Knowles, J. R.; Albery, W. J. *Acc. Chem. Res.* **1977**, *10*, 105–111.
- (2) Rieder, S. V.; Rose, I. A. *J. Biol. Chem.* **1959**, *234*, 1007–1010.
- (3) Go, M. K.; Koudelka, A.; Amyes, T. L.; Richard, J. P. *Biochemistry* **2010**, *49*, 5377–5389.
- (4) Richard, J. P.; Amyes, T. L. *Curr. Opin. Chem. Biol.* **2001**, *5*, 626–633.
- (5) Amyes, T. L.; Richard, J. P. In *Hydrogen-Transfer Reactions, Vol. 3, Biological Aspects I–II*; Hynes, J. T., Klinman, J. P., Limbach, H.-H., Schowen, R. L., Eds.; Wiley-VCH: Weinheim, 2007; Vol. 3, pp 949–973.
- (6) Richard, J. P. *Biochemistry* **1998**, *37*, 4305–4309.
- (7) Richard, J. P. *J. Am. Chem. Soc.* **1984**, *106*, 4926–4936.
- (8) Amyes, T. L.; O'Donoghue, A. C.; Richard, J. P. *J. Am. Chem. Soc.* **2001**, *123*, 11325–11326.

- (9) Tsang, W.-Y.; Amyes, T. L.; Richard, J. P. *Biochemistry* **2008**, *47*, 4575–4582.
- (10) Joseph-McCarthy, D.; Lolis, E.; Komives, E. A.; Petsko, G. A. *Biochemistry* **1994**, *33*, 2815–2823.
- (11) Joseph-McCarthy, D.; Rost, L. E.; Komives, E. A.; Petsko, G. A. *Biochemistry* **1994**, *33*, 2824–2829.
- (12) Jögl, G.; Rozovsky, S.; McDermott, A. E.; Tong, L. *Proc. Natl. Acad. Sci. U.S.A.* **2003**, *100*, 50–55.

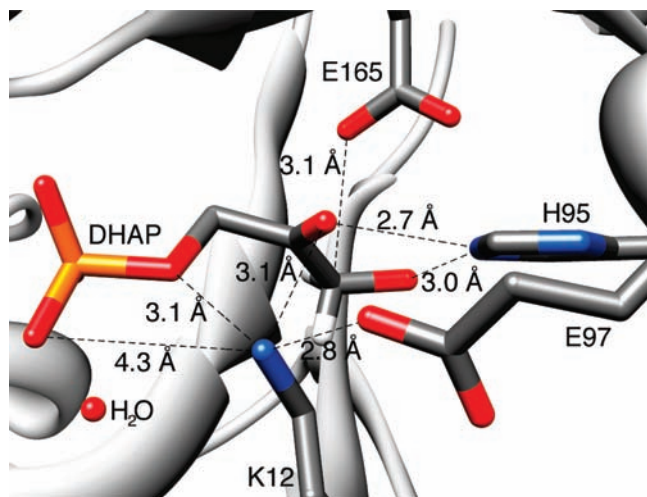


Figure 1. Structure of the active site of TIM, taken from the X-ray crystal structure of McDermott and co-workers (PDB entry 1NEY),¹² showing the distances between the ϵ -NH₃⁺ of Lys-12 and the functional groups of the enzyme-bound substrate DHAP.

ca. 0 kcal/mol at a standard state of 1 M have been reported for the formation of alkylammonium cation•phosphate anion pairs in water.^{13,14} One explanation for the much larger 7.8 kcal/mol interaction between the cationic side chain of Lys-12 of TIM and the anionic transition state for the isomerization of GAP is that the effectively intramolecular reaction of the side chain at TIM is favored entropically in comparison to the bimolecular reaction of alkylammonium cations as a result of the freezing of translational, rotational, and other motions of the tethered side chain. This reduces the entropic cost for formation of the transition state of the enzymatic reaction, compared with formation of the transition state for the corresponding bimolecular reaction in water.^{15,16}

We address here the importance of intramolecularity in the enhancement of the effect of the cationic side chain of Lys-12 at the active site of TIM, by examining “rescue” of the impaired catalytic activity of K12G mutant TIM by added ammonium cations (NH₄⁺ and RNH₃⁺). These cations are highly effective at restoring activity to K12G mutant TIM; however, their effect, at a standard state of 1 M, on the stability of the transition state for TIM-catalyzed isomerization of GAP is smaller than the 7.8 kcal/mol effect determined for the tethered cationic side chain of Lys-12. Our data provide *apparent* effective molarities (EMs) for the cationic side chain of Lys-12 at TIM ranging from 730 to 44 000 M that depend upon the choice of the activator cation.^{17,18} We present arguments that NH₄⁺ is the appropriate reference activator cation for calculation of the entropic advantage of the intramolecular alkylammonium side chain of Lys-12 at wildtype TIM.

Experimental Section

Materials. Wildtype and K12G mutant TIM from *Saccharomyces cerevisiae* were prepared and purified as described previously.³ Glycerol 3-phosphate dehydrogenase from rabbit muscle (GPDH)

was purchased from United States Biochemical, and bovine serum albumin (BSA) was from Roche.

D,L-Glyceraldehyde 3-phosphate diethyl acetal (barium salt), NADH (disodium salt), tetramethylammonium hydrogen sulfate, and *n*-propylamine hydrochloride were from Sigma. Ammonium chloride was from JT Baker. Ethylamine hydrochloride was from Fluka. Triethanolamine hydrochloride, 2-fluoroethylamine hydrochloride, and imidazole were from Aldrich. Methylamine hydrochloride, *n*-butylamine hydrochloride, and 2-methoxyethylamine were from TCI America. Imidazole was recrystallized from benzene. Water was obtained from a Milli-Q Academic purification system. All other commercially available chemicals were reagent grade or better and were used without further purification.

Preparation of Solutions. Solution pH was determined at 25 °C using an Orion model 720A pH meter equipped with a Radiometer pHC4006-9 combination electrode that was standardized at pH 7.00 and 10.00. Solutions of the following ammonium cations were prepared by dissolving the cationic form in water and adjusting the solution to pH 7.3 ± 0.2 using 1.0 M NaOH: 1.0 M NH₄⁺, 1.0 M CH₃NH₃⁺, 1.0 M CH₃CH₂NH₃⁺, 1.0 M CH₃-CH₂CH₂NH₃⁺, 1.0 M CH₃CH₂CH₂CH₂NH₃⁺, 0.125 M FCH₂-CH₂NH₃⁺, and 0.50 M (CH₃)₄N⁺. A solution of 1.0 M MeOCH₂-CH₂NH₃⁺ was prepared by adjusting a solution of the free amine base to pH 7.5 using concentrated HCl. Solutions of D,L-glyceraldehyde 3-phosphate were prepared by hydrolysis of the diethyl acetal and stored at -20 °C, as described previously.^{3,19,20}

Enzyme Assays. All enzyme assays were carried out at 25 °C. Changes in the concentration of NADH were calculated using an extinction coefficient of 6220 M⁻¹ cm⁻¹ at 340 nm. Enzymes were dialyzed at 4 °C against 20 mM triethanolamine (TEA) at pH 7.5, and dilute solutions of TIM were stabilized by the inclusion of 0.01% (0.1 mg/mL) BSA. The subunit concentration of K12G mutant yeast TIM in stock solutions was determined from the absorbance at 280 nm using an extinction coefficient of 2.55 × 10⁴ M⁻¹ cm⁻¹ that was calculated using the ProtParam tool available on the ExPASy server.^{21,22} GPDH was assayed by monitoring the oxidation of NADH by DHAP at 340 nm, as described previously.²⁰ The concentration of GAP in stock solutions of D,L-GAP was determined from the amount of NADH consumed during quantitative TIM-catalyzed isomerization of GAP to form DHAP that was coupled to the oxidation of NADH using GPDH.

The activities of wildtype and K12G mutant yeast TIM were determined by coupling the isomerization of GAP to the reduction of the product DHAP by NADH catalyzed by GPDH. The standard assay mixture (1.0 mL) contained 100 mM TEA at pH 7.5, 0.2 mM NADH, 5 mM D,L-glyceraldehyde 3-phosphate (D,L-GAP), and ca. 1 unit of GPDH at *I* = 0.10 (NaCl). A low background velocity *v*₀, due to both the nonenzymatic isomerization of GAP and the isomerization catalyzed by TIM that was present in the commercial preparation of GPDH, was determined over a period of 2–4 min. An aliquot of TIM was then added, and the total initial velocity *v*_{obsd} was determined by monitoring the reaction for an additional 5–10 min. The initial velocity of the TIM-catalyzed reaction was then calculated as *v*_i = *v*_{obsd} - *v*₀, where *v*₀ was generally ≤2% of the initial velocity *v*_{obsd}.

Rescue of K12G TIM by Ammonium Cations. The effect of added NH₄⁺ or RNH₃⁺ on the K12G mutant yeast TIM-catalyzed isomerization of GAP at 25 °C was examined using assay mixtures (1.0 mL) that contained 20 mM TEA buffer (pH 7.5, unless indicated otherwise), 20–80 mM RNH₃⁺, 0.2 mM NADH, 2–12

(13) Haake, P.; Prigodich, R. V. *Inorg. Chem.* **1984**, *23*, 457–462.

(14) Springs, B.; Haake, P. *Bioorg. Chem.* **1977**, *6*, 181–190.

(15) Page, M. I.; Jencks, W. P. *Proc. Natl. Acad. Sci. U.S.A.* **1971**, *68*, 1678–1683.

(16) Jencks, W. P. *Proc. Natl. Acad. Sci. U.S.A.* **1981**, *78*, 4046–4050.

(17) Kirby, A. *Adv. Phys. Org. Chem.* **1980**, 183–278.

(18) Barnett, S. A.; Amyes, T. L.; McKay Wood, B.; Gerlt, J. A.; Richard, J. P. *Biochemistry* **2010**, *49*, 824–826.

(19) O’Donoghue, A. C.; Amyes, T. L.; Richard, J. P. *Biochemistry* **2005**, *44*, 2610–2621.

(20) Go, M. K.; Amyes, T. L.; Richard, J. P. *Biochemistry* **2009**, *48*, 5769–5778.

(21) Gasteiger, E.; Gattiker, A.; Hoogland, C.; Ivanyi, I.; Appel, R. D.; Bairoch, A. *Nucleic Acids Res.* **2003**, *31*, 3784–3788.

(22) Gasteiger, E.; Hoogland, C.; Gattiker, A.; Duvaud, S.; Wilkins, M. R.; Appel, R. D.; Bairoch, A., Eds. *Protein Identification and Analysis Tools on the ExPASy Server*; Humana Press Inc.: Totowa, NJ, 2005.

mM D,L-GAP, ca. 1 unit of GPDH, and 0.06–1.5 μ M K12G TIM at $I = 0.1$ (NaCl), following the assay procedure described above. At the end of each assay, the protein was removed by ultrafiltration and the pH of the filtrate was determined and found to be within 0.01 unit of the initial pH of the TEA buffer.

Structures of K12G TIM Generated Using SYBYL. Structures of K12G mutant TIM in the presence and absence of alkylammonium cations were modeled using the molecular graphics software SYBYL version 7.3 (Tripos Inc., St. Louis, MO). The starting point for energy minimization was the X-ray crystal structure of yeast TIM (containing the W90Y, W157F, and W168(FTR) mutations) complexed with DHAP (Protein Data Bank entry 1NEY).¹² The K12G mutant was modeled by replacing the butylammonium side chain of Lys-12 by hydrogen. Formal charges for the protein and ligand were checked prior to assignment of Amber FF99^{23,24} charges for the protein and Gasteiger–Hückel charges for the ligand. The automated docking package FlexiDock, a module of SYBYL 7.3, was used to model the docking of $\text{CH}_3\text{CH}_2\text{NH}_3^+$ on the surface of the K12G mutant TIM•DHAP complex. The K12G mutant TIM•DHAP• $\text{CH}_3\text{CH}_2\text{NH}_3^+$ complex was generated by holding the ethylammonium cation as a fixed, energy minimized, aggregate during protein minimization by the Powell²⁵ algorithm, using the Tripos force field,²⁶ and with a gradient termination of 10 000 iterations as the convergence criterion. The docking of $\text{CH}_3\text{CH}_2\text{NH}_3^+$ at the K12G mutant TIM•DHAP complex did not significantly affect the coordinates of the protein complex.

Results

The slow nonenzymatic amine-catalyzed isomerization of GAP to form DHAP was observed in earlier studies using tertiary amines at pH 8.1–9.0.⁷ However, in the present work, there was no change in the initial velocity for conversion of GAP to DHAP in the absence of K12G TIM (v_0 , see Experimental Section) as the concentrations of ammonium cations were increased from 0 to 0.10 M at pH 7.5, 25 °C, and $I = 0.10$ (NaCl). This shows that, under our conditions, there is no detectable catalysis of the nonenzymatic isomerization reaction of GAP by either the free base or the conjugate acid of alkyl amines at neutral pH.

Figure 2A shows the effect of increasing concentrations of $\text{CH}_3\text{CH}_2\text{NH}_3^+$ on the initial velocity of the K12G mutant TIM-catalyzed isomerization of GAP at pH 7.5, 25 °C, and $I = 0.10$ (NaCl). The slopes of these linear correlations give the apparent second-order rate constant $(k_{\text{cat}}/K_{\text{m}})_{\text{obsd}}$ at the particular concentration of $\text{CH}_3\text{CH}_2\text{NH}_3^+$. Families of plots similar to that in Figure 2A were obtained for activation of K12G mutant TIM by NH_4^+ , CH_3NH_3^+ , $\text{CH}_3\text{CH}_2\text{CH}_2\text{NH}_3^+$, $\text{CH}_3\text{CH}_2\text{CH}_2\text{CH}_2\text{NH}_3^+$, $\text{MeOCH}_2\text{CH}_2\text{NH}_3^+$, and $\text{FCH}_2\text{CH}_2\text{NH}_3^+$. An increase in the concentration of $\text{CH}_3\text{CH}_2\text{CH}_2\text{NH}_3^+$ from 0.020 to 0.10 M at pH 7.5 has no effect (<10%) on the velocity of the wildtype TIM-catalyzed isomerization of GAP, so that the activation by $\text{CH}_3\text{CH}_2\text{CH}_2\text{NH}_3^+$ is specific for K12G mutant TIM.

Figure 2B shows the dependence of $(k_{\text{cat}}/K_{\text{m}})_{\text{obsd}}$ (determined as the slopes of the linear correlations in Figure 2A) for the K12G mutant TIM-catalyzed isomerization of GAP on the concentration of $\text{CH}_3\text{CH}_2\text{NH}_3^+$. The values of $(k_{\text{cat}}/K_{\text{m}})_{\text{obsd}}$ for the K12G TIM-catalyzed reactions determined at pH 7.0 fall on the same correlation line as those determined at pH 7.5,

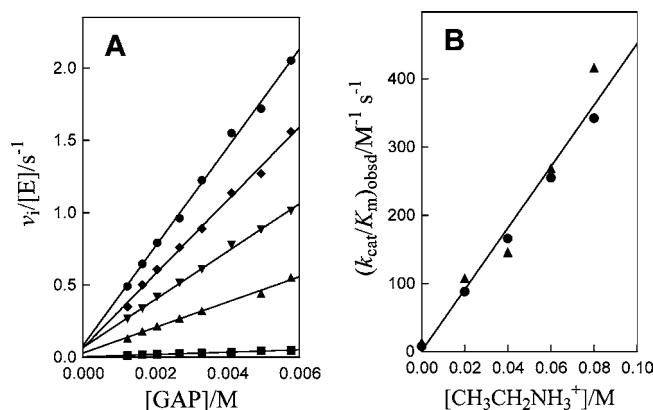


Figure 2. (A) Dependence of the initial velocity, normalized by the concentration of enzyme, of K12G yeast TIM-catalyzed isomerization of GAP at various concentrations of added $\text{CH}_3\text{CH}_2\text{NH}_3^+$ at pH 7.5, 25 °C, and $I = 0.10$ (NaCl). The slopes of these linear correlations give the apparent second-order rate constant $(k_{\text{cat}}/K_{\text{m}})_{\text{obsd}}$ at the particular concentration of $\text{CH}_3\text{CH}_2\text{NH}_3^+$. Key: (■) $[\text{EtNH}_3^+] = 0.0$ M; (▲) $[\text{EtNH}_3^+] = 0.020$ M; (▼) $[\text{EtNH}_3^+] = 0.040$ M; (◆) $[\text{EtNH}_3^+] = 0.060$ M; (●) $[\text{EtNH}_3^+] = 0.080$ M. (B) Dependence of the apparent second-order rate constant $(k_{\text{cat}}/K_{\text{m}})_{\text{obsd}}$ for isomerization of GAP catalyzed by K12G yeast TIM on the concentration of added $\text{CH}_3\text{CH}_2\text{NH}_3^+$. Key: (●) at pH 7.5; (▲) at pH 7.0.

where there is a 3-fold larger relative concentration of the basic form of the amine. This shows that there is no detectable rescue of K12G mutant TIM by the basic form of the amine, $\text{CH}_3\text{CH}_2\text{NH}_2$, so that the observed activation is due exclusively to rescue by $\text{CH}_3\text{CH}_2\text{NH}_3^+$. These data show that substitution of $\text{CH}_3\text{CH}_2\text{NH}_3^+$ for the side chain of Lys-12 rescues the activity of K12G mutant TIM.^{27–29} The following have no effect (<10%) on the velocity of the K12G mutant TIM-catalyzed isomerization of GAP at a constant ionic strength of 0.10, maintained with NaCl: (a) an increase in the concentration of triethanolamine buffer from 0.02 to 0.10 M; (b) an increase in the concentration of $(\text{CH}_3)_4\text{N}^+$ from 0 to 0.05 M.

Figure 3 shows the dependence of $(k_{\text{cat}}/K_{\text{m}})_{\text{obsd}}$ for the K12G mutant TIM-catalyzed isomerization of GAP on the concentration of several primary ammonium cations RNH_3^+ . The slopes of these linear correlations give the third-order rate constants for the activated reactions, $(k_{\text{cat}}/K_{\text{m}})_{\text{am}}/K_{\text{d}}$ ($\text{M}^{-2} \text{s}^{-1}$, Scheme 2), that are reported in Table 1.

Figure 4A shows the space-filling representation of the surface of yeast TIM complexed with DHAP in the region of Lys-12 that was prepared using the X-ray crystal structure data of McDermott and co-workers (PDB entry 1NEY).¹² The flexible loop 6 is colored cyan, and the surface waters have been removed for the sake of clarity. The side chain of Lys-12 extends across the protein surface with the charged $\epsilon\text{-NH}_3^+$ group oriented toward the phosphodianion group of bound DHAP. Figure 4B and C show, respectively, model structures of the K12G mutant TIM•DHAP complex and the same complex with $\text{CH}_3\text{CH}_2\text{NH}_3^+$ docked in the position of the excised side chain

(23) Case, D. A.; Cheatham, T. E., III; Darden, T.; Gohlke, H.; Luo, R.; Mertz, K. M., Jr.; Onufriev, A.; Simmerling, C.; Wang, B.; Woods, R. J. *J. Comput. Chem.* **2005**, 1668–1688.
 (24) Ponder, J. W.; Case, D. A. *Adv. Protein Chem.* **2003**, 66, 27–85.
 (25) Powell, M. J. D. In *Lecture Notes in Mathematics*; Griffiths, D. F., Ed.; Springer: Berlin/Heidelberg, 1984; Vol. 1066.
 (26) Clark, M.; Cramer, R. D., III; Opdenbosch, N. V. *J. Comput. Chem.* **1989**, 10, 982–1012.

(27) Peracchi, A. *Curr. Chem. Biol.* **2008**, 2, 32–49.
 (28) Toney, M. D.; Kirsch, J. F. *Science* **1989**, 243, 1485–1488.
 (29) Toney, M. D.; Kirsch, J. F. *Protein Sci.* **1992**, 1, 107–119.
 (30) Jencks, W. P.; Regenstein, J. In *Handbook of Biochemistry and Molecular Biology (Physical and Chemical Data)*, 3rd ed.; Fasman, G. D., Ed.; CRC Press: Cleveland, OH, 1976; Vol. 1, pp 305–351.
 (31) Kluger, R.; Hunt, J. C. *J. Am. Chem. Soc.* **1984**, 106, 5667–5670.

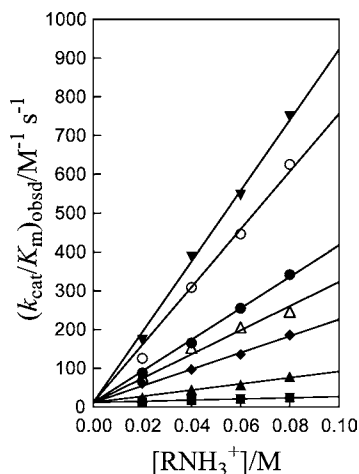


Figure 3. Dependence of $(k_{\text{cat}}/K_{\text{m}})_{\text{obsd}}$ for the K12G mutant TIM-catalyzed isomerization of GAP on the concentration of RNH_3^+ at pH 7.5, 25 °C, and $I = 0.10$ (NaCl). Key: (■) NH_4^+ ; (▲) CH_3NH_3^+ ; (◆) $\text{CH}_3\text{CH}_2\text{NH}_3^+$; (△) $\text{FCH}_2\text{CH}_2\text{NH}_3^+$; (○) $\text{CH}_3\text{CH}_2\text{NH}_3^+$; (◐) $\text{MeOCH}_2\text{CH}_2\text{NH}_3^+$; (▼) $\text{CH}_3\text{CH}_2\text{CH}_2\text{CH}_2\text{NH}_3^+$. The slopes of these linear correlation give the third-order rate constants $(k_{\text{cat}}/K_{\text{m}})_{\text{am}}/K_{\text{d}}$ for activation of K12G TIM by RNH_3^+ (Table 1).

Scheme 2

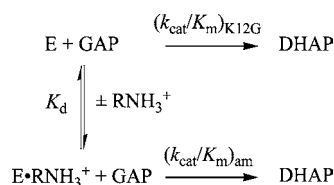


Table 1. Third-Order Rate Constants and Derived Rate Constant Ratios for Rescue of K12G Mutant Yeast TIM by NH_4^+ and RNH_3^+ ^a

RNH_3^+	pK_{a}	$(k_{\text{cat}}/K_{\text{m}})_{\text{am}}/K_{\text{d}}$ $\text{M}^{-2} \text{s}^{-1}$ ^b	$(k_{\text{cat}}/K_{\text{m}})_{\text{am}}/K_{\text{d}}$ $(k_{\text{cat}}/K_{\text{m}})_{\text{K12G}}$ M^{-1} ^c	$(k_{\text{cat}}/K_{\text{m}})_{\text{WT}}$ $(k_{\text{cat}}/K_{\text{m}})_{\text{am}}/K_{\text{d}}$ M^{d}
NH_4^+	9.3 ^e	150	13	44 000
CH_3NH_3^+	10.6 ^e	800	67	8300
$\text{CH}_3\text{CH}_2\text{NH}_3^+$	10.7 ^e	4100	340	1600
$\text{CH}_3\text{CH}_2\text{CH}_2\text{NH}_3^+$	10.6 ^e	2100	180	3100
$\text{CH}_3\text{CH}_2\text{CH}_2\text{CH}_2\text{NH}_3^+$	10.6 ^e	9100	760	730
$\text{MeOCH}_2\text{CH}_2\text{NH}_3^+$	9.7 ^f	7400	620	890
$\text{FCH}_2\text{CH}_2\text{NH}_3^+$	9.2 ^f	3100	260	2100
$(\text{CH}_3)_4\text{N}^+$		no effect at 0.05 M $(\text{CH}_3)_4\text{N}^+$		

^a For isomerization of GAP at pH 7.5, 25 °C, and $I = 0.10$ (NaCl).

^b Third-order rate constants for activation by the ammonium cation, calculated as the slopes of the linear correlations in Figure 3 with the intercept fixed at $(k_{\text{cat}}/K_{\text{m}})_{\text{K12G}} = 12 \text{ M}^{-1} \text{ s}^{-1}$ for reaction in the absence of RNH_3^+ . ^c Calculated using $(k_{\text{cat}}/K_{\text{m}})_{\text{K12G}} = 12 \text{ M}^{-1} \text{ s}^{-1}$ for the unactivated K12G TIM-catalyzed isomerization of GAP (ref 3). This is equal to $1/K_{\text{d}}$ (see eq 1). ^d Calculated using $(k_{\text{cat}}/K_{\text{m}})_{\text{WT}} = 6.6 \times 10^6 \text{ M}^{-1} \text{ s}^{-1}$ for wildtype yeast TIM-catalyzed isomerization of GAP (ref 3). This is the apparent EM of the side chain of Lys-12, using the given ammonium cation as the reference activator in the intermolecular reaction (see eq 3). ^e Data from the literature.³⁰ ^f Data from the literature.³¹

of Lys-12 that were generated starting from the structure for the TIM•DHAP complex using SYBYL (see Experimental Section).

Discussion

There have been many reports of rescue of the activity of mutant enzymes by small molecule analogues of the excised

amino acid side chain.²⁷ The data in Figures 2 and 3 show that primary ammonium cations RNH_3^+ can effectively replace the excised cationic side chain of Lys-12 and restore catalytic activity to K12G mutant TIM. Table 1 reports the third-order rate constants $(k_{\text{cat}}/K_{\text{m}})_{\text{am}}/K_{\text{d}}$ ($\text{M}^{-2} \text{ s}^{-1}$) for activation and rescue of the K12G TIM-catalyzed isomerization of GAP by several different RNH_3^+ (Scheme 2). These third-order rate constants were determined as the slopes of the plots of $(k_{\text{cat}}/K_{\text{m}})_{\text{obsd}}$ against $[\text{RNH}_3^+]$ shown in Figure 3. There is no detectable curvature in these plots for concentrations of cation activators up to 0.08 M. This shows that there is no significant formation of the binary $\text{E} \cdot \text{RNH}_3^+$ or the ternary $\text{E} \cdot \text{RNH}_3^+ \cdot \text{GAP}$ complexes under these conditions so that K12G TIM has only a weak affinity for RNH_3^+ .

The nature of the K12G mutation at TIM and of rescue of the mutant enzyme by RNH_3^+ are illustrated in Figure 4. Figure 4A shows the yeast TIM•DHAP complex¹² in which the closed flexible loop 6 (cyan) is wrapped around the phosphodianion group of DHAP.³² The side chain of Lys-12 lies on the protein surface, and its $\epsilon\text{-NH}_3^+$ group is anchored to the protein by a hydrogen bond with the carboxylate side chain of Glu-97 (Figure 1). The $\epsilon\text{-NH}_3^+$ group is 3.1 Å distant from both the bridging oxygen of the phosphodianion group and the carbonyl group of bound DHAP (Figure 1). The cationic side chain of Lys-12 interacts with the substrate phosphodianion group in the ground state, and the electrostatic interactions strengthen greatly on proceeding to the enediolate-like transition state where Lys-12 also interacts with the developing negative charge at the enolate oxygen.³ Figure 4B shows that the K12G mutation partly exposes the substrate to bulk solvent, while Figure 4C illustrates the docking of exogenous $\text{CH}_3\text{CH}_2\text{NH}_3^+$ with K12G TIM at the position of the excised side chain of Lys-12.

The location of the side chain of Lys-12 at the surface of TIM, where it is strongly solvated by water, favors effective rescue of K12G mutant TIM by added ammonium cations. By comparison, there should be a less effective rescue of mutants involving the side chains of charged residues buried inside protein cavities, where the wildtype amino acid side chains are “desolvated” in comparison to the side chain analog in water. In this case, the unfavorable barrier for desolvation of the side chain analog will contribute directly to the barrier for rescue. A careful examination of the relative effectiveness of rescue of mutations in different protein environments has the potential to provide insight into the catalytic importance of “desolvation” of catalytic side chains at the respective wildtype enzymes.

Substituent Effects on Rescue. The third-order rate constant $(k_{\text{cat}}/K_{\text{m}})_{\text{am}}/K_{\text{d}}$ for activation of the K12G mutant TIM-catalyzed isomerization of GAP increases from 150 to 800 to 4100 $\text{M}^{-2} \text{ s}^{-1}$ when a H at NH_4^+ is replaced first by a methyl group to give CH_3NH_3^+ and then by an ethyl group to give $\text{CH}_3\text{CH}_2\text{NH}_3^+$ (Table 1). This is consistent with stabilization of the transition state by hydrophobic interactions between the enzyme and the side chain R of the ammonium cation activator RNH_3^+ , resulting in an increase in the affinity of the cation for K12G mutant TIM (decrease in K_{d} and K_{d}^{\ddagger} , Scheme 3). Lengthening of the side chain at RNH_3^+ to 3 and then to 4 carbons results in first a decrease in $(k_{\text{cat}}/K_{\text{m}})_{\text{am}}/K_{\text{d}}$ to 2100 $\text{M}^{-2} \text{ s}^{-1}$ and then an increase to 9100 $\text{M}^{-2} \text{ s}^{-1}$ (Table 1). These changes reflect subtle effects of the chain length of RNH_3^+ on the stability of the protein• RNH_3^+ complex. There is a strong specificity for rescue by

(32) Pompliano, D. L.; Peyman, A.; Knowles, J. R. *Biochemistry* **1990**, *29*, 3186–3194.

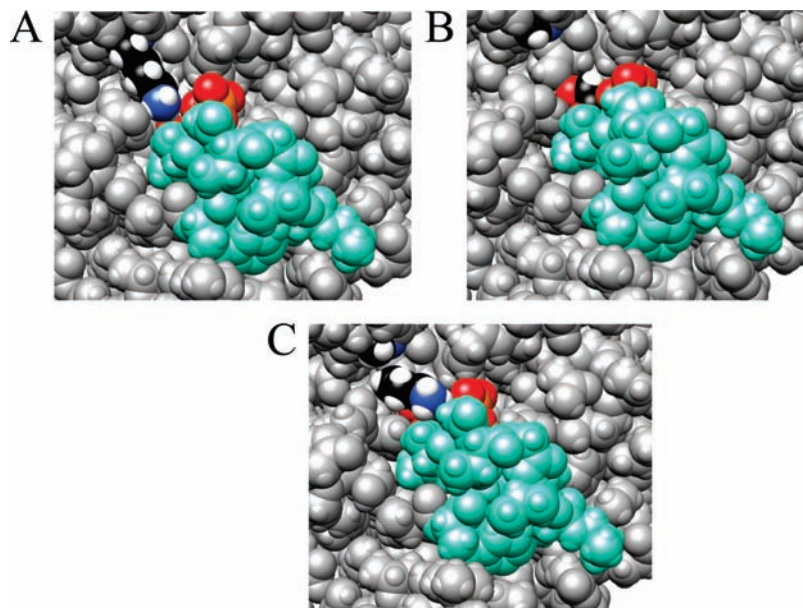


Figure 4. Space-filling representations of the surface of TIM complexed with DHAP in the region of Lys-12, generated as described in the Experimental Section. The flexible loop 6 is shown in cyan; the alkylammonium side chain of Lys-12 at the wildtype enzyme is colored black (carbon), white (hydrogen), and dark blue (nitrogen); and the substrate DHAP is colored black, white, red (oxygen), and orange (phosphorus). (A) Wildtype yeast TIM (PDB entry 1NEY).¹² (B) K12G mutant TIM. (C) K12G mutant TIM with $\text{CH}_3\text{CH}_2\text{NH}_3^+$ docked in the position of the excised side chain of Lys-12. The surface waters have been removed for the sake of clarity.

primary ammonium cations. There is no significant rescue of the K12G TIM-catalyzed isomerization of GAP by the quaternary ammonium ion $(\text{CH}_3)_4\text{N}^+$ or by the conjugate acid of triethanolamine, a tertiary ammonium cation.

Table 1 includes limited data relevant to the effect of changing the $\text{p}K_a$ of RNH_3^+ on the activation of K12G mutant TIM. Similar third-order rate constants $(k_{\text{cat}}/K_m)_{\text{am}}/K_d$ were determined for rescue of K12G mutant TIM by $\text{CH}_3\text{CH}_2\text{CH}_2\text{CH}_2\text{NH}_3^+$ and $\text{MeOCH}_2\text{CH}_2\text{NH}_3^+$, whose side chains are nominally of the same length but whose $\text{p}K_a$ values differ by 0.9 units. Replacement of the CH_3 group of $\text{CH}_3\text{CH}_2\text{CH}_2\text{NH}_3^+$ by F to give $\text{FCH}_2\text{CH}_2\text{NH}_3^+$ results in a 1.4 unit decrease in $\text{p}K_a$ and a small ca. 50% increase in $(k_{\text{cat}}/K_m)_{\text{am}}/K_d$, while replacement of the terminal H of $\text{CH}_3\text{CH}_2\text{NH}_3^+$ by F to give $\text{FCH}_2\text{CH}_2\text{NH}_3^+$ results in a 1.5 unit decrease in $\text{p}K_a$ but a ca. 30% decrease in $(k_{\text{cat}}/K_m)_{\text{am}}/K_d$. In short, there is no strong dependence of $(k_{\text{cat}}/K_m)_{\text{am}}/K_d$ for rescue of K12G mutant TIM on the $\text{p}K_a$ of RNH_3^+ . These results are consistent with the conclusion that the Brønsted parameter α for rescue by ammonium cations is close to zero. Therefore, there is little or no formal proton transfer from the cationic activator to the developing enolate oxygen in the transition state, so that the ammonium cation is fully protonated at the transition state for the TIM-catalyzed isomerization of GAP. The results are inconsistent with the prediction of a computational study that full proton transfer from the $\epsilon\text{-NH}_3^+$ group of Lys-12 to the substrate phosphodianion group precedes enolization of the substrate,³³ because the coupling of this proton transfer to catalysis would require a Brønsted coefficient of $\alpha = 1.0$ for activation of K12G mutant TIM by ammonium cations.

TIM in Pieces. The side chain of Lys-12 at wildtype TIM sits at the surface of the protein where it is exposed to solvent (Figure 4A).^{12,34} Deletion of this side chain “in silico” leaves

a gap at the K12G mutant, and it would appear that there is no impediment to the “binding” of NH_4^+ and RNH_3^+ . The ability of primary ammonium cations to activate and rescue K12G mutant TIM and the advantage of covalent attachment of the cationic activator to the enzyme can be quantified by two parameters that are related by the overall effect of the K12G mutation on the TIM-catalyzed isomerization of GAP (Table 1).

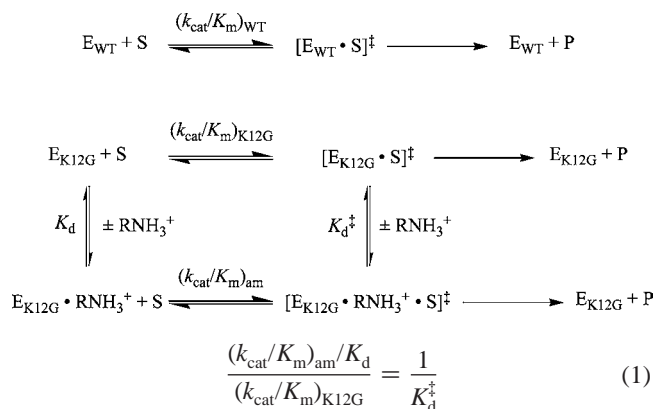
First, the ratio of the third-order rate constant $(k_{\text{cat}}/K_m)_{\text{am}}/K_d$ for rescue of K12G mutant TIM by RNH_3^+ and the second-order rate constant $(k_{\text{cat}}/K_m)_{\text{K12G}}$ for the *unactivated* K12G mutant TIM-catalyzed isomerization provides a measure of the stabilization of the transition state for the mutant enzyme-catalyzed reaction by a standard state of 1 M activator cation (Scheme 3 and Table 1). Equation 1 shows the simple relationship between this ratio and the *association* constant $1/K_d^\ddagger$ for *binding* of RNH_3^+ to the transition state for the K12G mutant TIM-catalyzed isomerization of GAP. Equation 2 defines the *stabilization* of the transition state by interactions with the cationic activator at a standard state of 1 M, $\Delta G_{\text{RNH}_3^\ddagger}$.

Second, the ratio of the second-order rate constant $(k_{\text{cat}}/K_m)_{\text{WT}}$ for the wildtype TIM-catalyzed reaction and the third-order rate constant $(k_{\text{cat}}/K_m)_{\text{am}}/K_d$ for rescue of K12G mutant TIM by RNH_3^+ gives the effective molarity (EM, eq 3) of the ammonium side chain of Lys-12 at the wildtype enzyme (Table 1).¹⁷ Equation 3 shows that the EM is also given by the product of the *overall* effect of the K12G mutation and the dissociation constant for RNH_3^+ from the transition state, K_d^\ddagger (Scheme 3). The observed EM depends partly or entirely on the entropic advantage of the effectively intramolecular interaction of the $\epsilon\text{-NH}_3^+$ side chain of Lys-12 at wildtype TIM compared with the bimolecular activation of K12G mutant TIM by RNH_3^+ (Scheme 3). Table 1 reports the various values of EM for the cationic side chain of Lys-12 that were calculated from the data for several different ammonium cation activators.

(33) Guallar, V.; Jacobson, M.; McDermott, A.; Friesner, R. A. *J. Mol. Biol.* **2004**, *337*, 227–239.

(34) Kursula, I.; Wierenga, R. K. *J. Biol. Chem.* **2003**, *278*, 9544–9551.

Scheme 3



$$\Delta G_{\text{RNH}_3}^{\ddagger} = -RT \ln(1/K_{\text{d}}^{\ddagger}) \quad (2)$$

$$\text{EM} = \frac{(k_{\text{cat}}/K_{\text{m}})_{\text{WT}} K_{\text{d}}}{(k_{\text{cat}}/K_{\text{m}})_{\text{am}}} = \frac{(k_{\text{cat}}/K_{\text{m}})_{\text{WT}} K_{\text{d}}^{\ddagger}}{(k_{\text{cat}}/K_{\text{m}})_{\text{K12G}}} \quad (3)$$

$$\Delta G_{\text{S}}^{\ddagger} = (\Delta G_{\text{K12G}}^{\ddagger} + \Delta G_{\text{RNH}_3}^{\ddagger}) - \Delta G_{\text{WT}}^{\ddagger} = RT \ln \text{EM} \quad (4)$$

$$\frac{(k_{\text{cat}}/K_{\text{m}})_{\text{WT}}}{(k_{\text{cat}}/K_{\text{m}})_{\text{K12G}}} = \text{EM}/K_{\text{d}}^{\ddagger} = 5.5 \times 10^5 \quad (5)$$

$$\Delta G_{\text{K12G}}^{\ddagger} - \Delta G_{\text{WT}}^{\ddagger} = \Delta G_{\text{S}}^{\ddagger} - \Delta G_{\text{RNH}_3}^{\ddagger} = 7.8 \text{ kcal/mol} \quad (6)$$

Equation 4 defines the *connection energy* $\Delta G_{\text{S}}^{\ddagger}$ as the difference between the activation barriers for the isomerization reaction catalyzed by K12G TIM in the presence of 1 M RNH_3^+ , $\Delta G_{\text{K12G}}^{\ddagger} + \Delta G_{\text{RNH}_3}^{\ddagger}$, and by the wildtype enzyme, $\Delta G_{\text{WT}}^{\ddagger}$. There is a simple direct correspondence between this connection energy and EM (eq 4). Equation 5 shows that there is an inverse relationship between the EM calculated for a given reference cation activator and its transition state dissociation constant K_{d}^{\ddagger} , because their ratio is equal to the *constant* 5.5×10^5 -fold overall effect of the K12G mutation on $k_{\text{cat}}/K_{\text{m}}$ for isomerization of GAP. Equation 6, the logarithmic equivalent of eq 5, partitions the constant 7.8 kcal/mol overall effect of the K12G mutation on the activation barrier for isomerization of GAP into the part that can be *rescued* by 1 M activator, $-\Delta G_{\text{RNH}_3}^{\ddagger}$, and the observed advantage to the intramolecular reaction, $\Delta G_{\text{S}}^{\ddagger}$.

Connection Energy. The connection energy $\Delta G_{\text{S}}^{\ddagger}$ (eq 4) is the *empirical* transition state stabilization obtained by connecting the two enzyme pieces K12G and RNH_3^+ .¹⁶ In the simplest case, this connection energy would be largely an entropy term and a function of the change in the overall translational and rotational entropy observed when a free ammonium cation activator in a bimolecular reaction is *immobilized* at the enzyme active site. However, $\Delta G_{\text{S}}^{\ddagger}$ may also include an enthalpic component, in the case where there is an enthalpic advantage or disadvantage to the intermolecular reaction that does not contribute to the barrier for the wildtype enzyme-catalyzed reaction. For example:

(1) The *unfavorable* enthalpic barrier for desolvation of the side chain analog upon binding to the mutant enzyme may add to the barrier to intermolecular rescue, but by definition it cannot contribute to the barrier for the wildtype enzyme-catalyzed reaction because the price for desolvation of the side chain is *paid* during protein folding. In the limiting case, where the

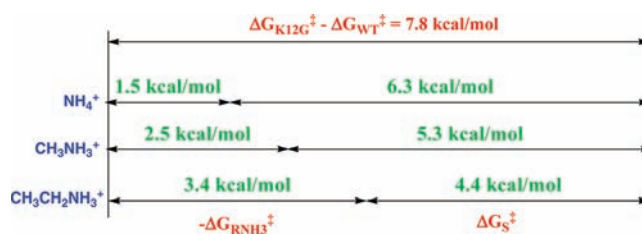


Figure 5. A comparison of the binding energy of primary ammonium cations to the transition state for K12G mutant TIM-catalyzed isomerization of GAP, $-\Delta G_{\text{RNH}_3}^{\ddagger}$, and the apparent transition state stabilization obtained from connecting these activators to the mutant enzyme, $\Delta G_{\text{S}}^{\ddagger}$. The sum of these terms is equal to the overall stabilization of the transition state for the wildtype TIM-catalyzed isomerization of GAP by interaction with the cationic side chain of Lys-12, $\Delta G_{\text{K12G}}^{\ddagger} - \Delta G_{\text{WT}}^{\ddagger} = 7.8$ kcal/mol (eq 6).

barrier to desolvation is so large that rescue becomes poor or negligible, K_{d}^{\ddagger} will be very large and hence there will be a correspondingly large advantage to the reaction of the tethered protein side chain (large EM, eq 5). Such large EMs will include the unfavorable enthalpic barrier to the intermolecular reaction and will therefore *overestimate* the entropic advantage to the intramolecular reaction.

(2) *Stabilizing* enthalpic binding interactions between the activator and the enzyme may reduce the barrier to intermolecular rescue, but by definition they cannot affect the barrier to the wildtype enzyme-catalyzed reaction because the interactions between the side chain and the protein are already present at the ground state enzyme. In the limiting case where the activator binds very tightly to the enzyme, K_{d}^{\ddagger} will be very small and hence there will be a correspondingly small advantage to the reaction of the tethered protein side chain (small EM, eq 5). Such small EMs will include the favorable enthalpic barrier to the intermolecular reaction and will, therefore, *underestimate* the entropic advantage to the intramolecular reaction.

Figure 5 shows that the advantage of tethering NH_4^+ , CH_3NH_3^+ , and $\text{CH}_3\text{CH}_2\text{NH}_3^+$ to the enzyme, $\Delta G_{\text{S}}^{\ddagger}$, becomes progressively smaller as the transition state protein•activator complex is stabilized enthalpically by interactions between TIM and the alkyl side chain of the activator (decrease in K_{d}^{\ddagger}). We propose that the limiting value of $\Delta G_{\text{S}}^{\ddagger} = 6.3$ kcal/mol for activation of TIM by NH_4^+ provides a fair estimate of the entropic advantage of the effectively intramolecular interaction of the side chain of Lys-12 at wildtype TIM over the intermolecular interaction of an ammonium cation activator and the K12G mutant. The larger connection energy of $\Delta G_{\text{S}}^{\ddagger} = 6.3$ kcal/mol for NH_4^+ compared with $\Delta G_{\text{S}}^{\ddagger} = 5.3$ kcal/mol for CH_3NH_3^+ calculated from the data in Table 1 might reflect the larger energetic cost of “desolvation” of NH_4^+ compared with the simple primary ammonium cation. However, the further decrease to $\Delta G_{\text{S}}^{\ddagger} = 4.4$ kcal/mol for activation by $\text{CH}_3\text{CH}_2\text{NH}_3^+$ suggests that these effects are likely related to stabilization of the TIM•activator complex by interactions between the mutant enzyme and the alkyl group of RNH_3^+ , rather than to the effects of solvation. We cannot rigorously evaluate the contribution of the barrier to desolvation of NH_4^+ to K_{d}^{\ddagger} for activation by NH_4^+ but suggest that this is small. In aqueous solution NH_4^+ participates in five hydrogen bonds with water molecules in the first hydration layer.³⁵ The price of desolvation of the first water during the binding of NH_4^+ to K12G mutant TIM should be recovered through formation of a hydrogen bond to the carboxylate side chain of Glu-97 (Figure 1). It is not known

(35) Jorgensen, W. L.; Gao, J. *J. Phys. Chem.* **1986**, *90*, 2174–2182.

whether loss of the further water molecules of solvation from NH_4^+ is required for effective rescue. However, the small and apparently “normal” ca. 1 kcal/mol effect of the methyl substituent on $-\Delta G_{\text{RNH}_3^\ddagger}$ for activation by CH_3NH_3^+ (Figure 5) suggests that the requirement for desolvation that accompanies binding of NH_4^+ is no greater than that for the desolvation of CH_3NH_3^+ . If there is a significant barrier to the desolvation of NH_4^+ in the intermolecular reaction that is not observed in the reaction of wildtype TIM, then the apparent 6.3 kcal/mol advantage to connection of the cationic activator to TIM (Figure 5) will overestimate the advantage of the intramolecular interaction of the $\epsilon\text{-NH}_3^+$ of the side chain of Lys-12.

Other Enzymes. Orotidine 5'-monophosphate decarboxylase (OMPDC) catalyzes the decarboxylation of orotidine 5'-monophosphate (OMP) to give uridine 5'-monophosphate (UMP) through an unstable vinyl carbanion intermediate.^{36,37} The guanidinium cation side chain of Arg-235 (numbering for the enzyme from yeast) forms a bidentate ion pair with the phosphodianion group of the bound intermediate analog 6-hydroxyuridine 5'-monophosphate, and its position adjacent to the phosphate gripper loop 7 of OMPDC resembles the positioning of Lys-12 adjacent to loop 6 of TIM (Figure 4A).³⁸ The R235A mutation at yeast OMPDC results in a $\Delta G_{\text{R235A}^\ddagger} - \Delta G_{\text{WT}^\ddagger} = 5.8$ kcal/mol destabilization of the transition state for OMPDC-catalyzed decarboxylation of OMP,¹⁸ which is smaller than the 7.8 kcal/mol effect of the K12G mutation at TIM.³ One reason for the difference is that Arg-235 at OMPDC lies further from the developing negative charge in the transition state at C-6 of the pyrimidine ring of OMP, compared with the relatively close proximity of Lys-12 at TIM and the developing negative charge at the enediolate formed from deprotonation of GAP or DHAP.

There is a larger stabilization of the transition state for R235A mutant OMPDC by 1 M guanidinium cation, $\Delta G_{\text{Gua}^\ddagger} = -2.8$ kcal/mol, compared with $\Delta G_{\text{RNH}_3^\ddagger} = -1.5$ kcal/mol for the activation of K12G mutant TIM by 1 M NH_4^+ (Figure 5), despite the apparently smaller stabilizing interaction of the guanidinium cation side chain of Arg-235 at OMPDC (5.8 kcal/mol effect of the R235A mutation) than that of the alkylammonium cation side chain of Lys-12 at TIM (7.8 kcal/mol effect of the K12G mutation). This difference is due partly or entirely to the larger favorable enthalpy change for binding of the bidentate guanidinium cation to the [OMPDC•OMP] complex ($K_d = 0.05$ M)¹⁸ than for binding of NH_4^+ to the TIM•GAP complex ($K_d \gg 0.1$ M, *vide infra*). However, there is a smaller connection energy of $\Delta G_{\text{S}^\ddagger} = 5.8 + \Delta G_{\text{Gua}^\ddagger} = 3.0$ kcal/mol (see eq 4) for covalent tethering of the R235A OMPDC and guanidinium cation pieces compared with $\Delta G_{\text{S}^\ddagger} = 6.3$ kcal/mol for covalent tethering of the K12G TIM and NH_4^+ pieces.

The difference in these values of $\Delta G_{\text{S}^\ddagger}$ for OMPDC and TIM reflects the wholly empirical nature of $\Delta G_{\text{S}^\ddagger}$ and hence the difficulty in assessing the *quality* of the reference bimolecular reaction of the activator cation used in its determination via eqs 3 and 4. The true *entropic* advantage of the intramolecular reaction of the whole enzyme will be *smaller* than these apparent advantages when there is a barrier to the bimolecular reference

reaction, such as desolvation of the activator cation, that does not contribute to the barrier for the intramolecular reaction. The *entropic* advantage of the intramolecular reaction will be *larger* than these apparent advantages when there is a driving force for the bimolecular reference reaction that does not contribute to the intramolecular reaction, such as stabilizing hydrophobic interactions of the activator with the protein. There can be little such stabilization of the complex between NH_4^+ and K12G TIM, and we therefore propose that $\Delta G_{\text{S}^\ddagger} = 6.3$ kcal/mol for connection of the K12G TIM and NH_4^+ pieces provides a fair estimate of the entropic advantage to the reaction of the whole enzyme. The rescue of R57G mutant ornithine transcarbamylase³⁹ and of R127A mutant carboxypeptidase⁴⁰ by guanidine derivatives has been reported. It would be useful to extend the present work and to determine values for $\Delta G_{\text{S}^\ddagger}$ and $\Delta G_{\text{Gua}^\ddagger}$ for the reactions of these enzyme pieces.

Conclusions and Speculation

The 7.8 kcal/mol stabilization of the transition state for the TIM-catalyzed isomerization of GAP by the cationic side chain of Lys-12 is critical for the observation of robust catalysis.³ TIM is by some criteria a “perfect” enzyme^{1,41} so that 7.8 kcal/mol may be approaching an upper limit for stabilization of a transition state trianion by electrostatic interaction with a side chain monocation. The $\epsilon\text{-NH}_3^+$ group of Lys-12 at the surface of TIM is directed toward both the phosphodianion and carbonyl groups of bound DHAP (Figure 4A) while the reacting functional groups of the substrate are buried in the protein interior,^{12,34} where the local dielectric constant is expected to be smaller than that of water.^{42–44} This reduction in the local dielectric constant will have the effect of enhancing stabilizing electrostatic interactions in the transition state for both the intramolecular and intermolecular reactions.⁴⁵ The relatively large 1.5 kcal/mol stabilization of the transition state for isomerization of GAP catalyzed by K12G mutant TIM by 1.0 M NH_4^+ is consistent with such an enhancement of electrostatic stabilization.

There are several related proposals in the literature that attempt to explain the large advantage of enzymes over small molecules as catalysts of chemical reactions. It has been suggested that the catalytic residues at enzyme active sites are “preorganized for reactions”⁴⁶ or “optimally aligned” for catalysis¹² and that “electrostatic stabilization” of the transition state for enzymatic reactions is favored because of the small energetic cost of “reorganization” at the preorganized environment of an enzyme active site.⁴⁷ These models each predict a greater stabilization of the transition states for enzymatic reactions by effective *intramolecular* electrostatic interactions between charged amino acid side chains and the enzyme-bound transition state, compared with the stabilization observed in the corresponding intermolecular reaction of the amino acid side chain analog.

- (36) Amyes, T. L.; Wood, B. M.; Chan, K.; Gerlt, J. A.; Richard, J. P. *J. Am. Chem. Soc.* **2008**, *130*, 1574–1575.
 (37) Toth, K.; Amyes, T. L.; Wood, B. M.; Chan, K.; Gerlt, J. A.; Richard, J. P. *J. Am. Chem. Soc.* **2007**, *129*, 12946–12947.
 (38) Miller, B. G.; Hassell, A. M.; Wolfenden, R.; Milburn, M. V.; Short, S. A. *Proc. Natl. Acad. Sci. U.S.A.* **2000**, *97*, 2011–2016.

- (39) Rynkiewicz, M. J.; Seaton, B. A. *Biochemistry* **1996**, *35*, 16174–16179.
 (40) Phillips, M. A.; Hedstrom, L.; Rutter, W. J. *Protein Sci.* **1992**, *1*, 517–521.
 (41) Albery, W. J.; Knowles, J. R. *Biochemistry* **1976**, *15*, 5627–5631.
 (42) Antosiewicz, J.; McCammon, J. A.; Gilson, M. K. *Biochemistry* **1996**, *35*, 7819–7833.
 (43) Sham, Y. Y.; Muegge, I.; Warshel, A. *Biophys. J.* **1998**, *74*, 1744–1753.
 (44) Georgescu, R. E.; Alexov, E. G.; Gunner, M. R. *Biophys. J.* **2002**, *83*, 1731–1748.
 (45) Richard, J. P.; Amyes, T. L. *Bioorg. Chem.* **2004**, *32*, 354–366.
 (46) Cannon, W. R.; Benkovic, S. J. *J. Biol. Chem.* **1998**, *273*, 26257–26260.
 (47) Warshel, A. *J. Biol. Chem.* **1998**, *273*, 27035–27038.

Our best estimate for the entropic advantage to reaction of the ϵ -NH₃⁺ of the side chain of Lys-12 at wildtype TIM, compared to the bimolecular reaction of an ammonium cation, is 6.3 kcal/mol. The summation of such large entropic advantages for a pair or trio of catalytic side chains would go a long way toward rationalizing the large rate accelerations observed for some enzyme catalysts.^{15,16} One obvious challenge to designing proteins with enzyme-like catalytic activities will be the engineering of amino acid side chains that exhibit the high effective molarities of catalytic side chains observed for catalysis

by OMPDC,¹⁸ TIM (this work), mandelate racemase,⁴⁸ and, presumably, other enzyme catalysts.

Acknowledgment. We acknowledge the National Institutes of Health Grant GM39754 for generous support of this work. We thank Professor Gerald Koudelka for help with SYBYL and generation of the structures of K12G TIM.

JA106104H

(48) Bearne, S. L.; Wolfenden, R. *Biochemistry* **1997**, *36*, 1646–1656.